Journal of Applied Fluid Mechanics, Vol. 10, No. 1, pp. 343-352, 2017.
Available online at www.jafmonline.net, ISSN 1735-3572, EISSN 1735-3645.
DOI: 10.18869/acadpub.jafm.73.238.25759

Experimental and Numerical Investigation of High Speed Swimmer Motion Drag Force in Different Depths from Free Surface

M. R. Sadeghizadeh[1†], B. Saranjam[2] and R. Kamali[3]

[1]*Department of Hydro-Aerodynamic Research Center of Malek-e Ashtar University of Technology, Shiraz, Iran*
[2] *of Air-Naval Complex of Malek-e Ashtar University of Technology, Shiraz, Iran*
[3] *School of Mechanic Engineering, Shiraz University, Shiraz, Iran*

†*Corresponding Author Email: Mr_sadeghizadeh@yahoo.com*

(Received October 28, 2015; accepted August 20, 2016)

ABSTRACT

In this study, the drag force exerted on swimmer body is investigated by computational fluid dynamic (CFD) and then the results validity are compared with towing tank experiments. The main target of this research is swimmer thruster power evaluation to reach the high speed motion underwater. In the last decade, the low speed swimmer motion has been studied by researchers for sport purposes and improvement of diving time record, while in this research authors have tried to increase swimmer speed up to 8 ms^{-1} by use of electrical thruster system. The numerical simulations have been done by computational fluid dynamics considering three dimensional two phase turbulent flow in the base of Volume of Fluid (VOF) method. The geometry of the swimmers' bodies was generated by 3-D scanning and image modeling of real swimmers in experimental diving test. Different turbulent models could be applied in specific case but the favorable one (k–ε method) is selected to estimate the forces on the swimmers. The experiments were programed by five swimmers and one mannequin for different depths and speeds. The numerical simulation results showed a good agreement with the experimental output data up to 8 ms^{-1} but more speed test results were not accessible because of lab limitations. The results showed whatever swimmer go to deeper depths up to certain value the drag force exerted to him will be reduced. This work introduced asseveration about maximum swimmer speed test worldwide that is twice the other work heretofore.

Keywords: Swimmers drag force; CFD; Swimmers towing test.

NOMENCLATURE

A_f	frontal area
C_1, C_2	closure coefficient of k-ε method
C_μ	viscosity modification factor
d_e	equivalent diameter
D_t	total drag force
F_r	Froude number
g	gravity
h_s	swimming depth
k	turbulent kinetic energy per unit mass
L	swimmer characteristic length
$\bar{P}$	pressure time average value
P_r	required power
P_i	installed power
Re	Reynolds number
U	swimmer velocity
$U_i(t)$	flow instantaneous velocity value
$\bar{U}$	velocity time average value
u_i	X- velocity component
u_j	Y- velocity component
v_f	volume of fluid
δ_{ij}	Kroneker delta
η_p	propulsion efficiency
μ	dynamic viscosity
μ_t	turbulent viscosity
ρ	water
υ	kinematic viscosity
σ_k - σ_ε	closure coefficient of k-ε method
ε	dissipation rate of the turbulent kinetic energy per unit mass

1. INTRODUCTION

It is undoubted that the improvement of swimmer speed motion is currently and the tendency to increase it has been considered notwithstanding of water environment limitations. The investigation of

drag force is main problem of this subject that is composed of skin-friction, profile and wave drag. Generally, the contribution of skin friction drag relative to others components is low enough so more focus has been considered to profile and wave components. Though, many research strategies have been planned to reduce drag in the requirement for higher swimmer speed recently. According as improved fundamental mechanisms of swimming understanding the concept of using different design of swimmer scooters will be executed to pass higher speed motion for more underwater traveling. Many researchers tried to present experimental and numerical methods for predicting drag force to estimate of swimmer ability that should be resisted against it. The researchers have been revealed the difficulties involved in conducting of swimmer towing experiments. It was necessary to choose a safe method of experiment with under controlled condition. Recently the evaluation of arm and hand swimming propulsion has been investigated by applying numerical technique of computational fluid dynamics. In addition, the details of fluid flow around the hand and arm have been illustrated. The possibility of this work has been presented by Bixler and Schloder (1996) when they used a 2D CFD analysis to evaluate the effects of accelerating of a flat circular plate through water. Also, they showed that 3D CFD was applicable to analysis of an actual swimmer. Several researchers have been focused on results of numerical simulations because of the complexity and high cost of experiments.

Bixler and Riewald (2002) used the computational fluid dynamics technique to investigate the flow around the hand/forearm of a swimmer. They have been used the numerical simulation to calculate the forces and related hydrodynamic coefficients for several swimmer angles of attack. The standard k–ε model of turbulent has been selected for their studies and applied a non-equilibrium wall function flow treatment in the vicinity of the body surface in order to increase solution accuracy. The same model has been used by Rouboa *et al.* (2006) for calculating the drag and lift force coefficients of the hand/forearm, both under steady and unsteady flow conditions and estimated the hand/forearm acceleration effect on the propulsive force magnitude in their simulation.

The unsteady CFD was carried out to consider the effects of acceleration and transient motions of the hand in predicting swimmer's thrust by Sato and Hino (2003) in another research. Gardano and Dabnichki (2006) measured experimentally and numerically the drag and lift forces for a model of the whole human arm. This work constituted an important potential for the use of unsteady CFD simulation of swimmer motion underwater. On the other hand, Vennell *et al.* (2006) focused on wave drag of swimmers. They followed their research by towing a mannequin in different speed from about 0.4 to 2.5ms^{-1} and up to 1 meter depth. They showed that the total drag at the surface is up to 2.4 times of drag when had been immersed fully.

Cohen (2009) simulated the human swimming by using smoothed particle hydrodynamics. He overcame many difficulties according to his technique such as combination of turbulent flow and complexity of free surface motion including water splash and entrainment of gas and rapid deforming of swimmer geometry. The surface of swimmers' body was generated by laser scanning. The simulations have been followed by deformation of the surface mesh for speed of 1.0 and 1.5 ms^{-1}. He presented his simulation based on *SPH* capabilities.

In another research in this year the effect of body position on drag coefficient during submerged gliding in swimming has been simulated by Marinho *et al.* (2009). They used k–ε model of turbulent for a three-dimensional male swimmer and have been presented simulation for flow velocities between 1.6 to 2.0 ms^{-1}. Also, the hydrodynamic characteristics analysis of swimmer hand and forearm has been studied with 3D-CFD in another research (2011) by them.

Whereas there are many turbulence models for numerical computation but for selecting of suitable one has been studied by Zaidi *et al* (2010). They showed that standard k-ε and k-ω models might be used for numerical simulation but the second one is better and it has more accurate results.

The analysis of wall shear stress around a swimmer has been studied by Popa *et al.* (2011). They also used k-ω model in 3D-CFD numerical simulation for calculating wall shear stresses near body and showed that the values will be increased in rigid body regions like head and shoulders of swimmer. Prediction of passive and active drag in swimming has been done by Webb (2011). He combined the empirical methods and theoretical analysis to predict passive resistance in the speed range up to 2 ms^{-1} and the results have been compared with experimental tests. The comparison has been made between the data derived from Velocity Perturbation Method and Naval Architecture based approach in predicting active drag.

Ramos (2012) has been presented a three dimensional CFD analysis for simulating the effect of body positions on drag during the streamlined glide too. The purpose of that research was investigated the body position effects on drag during the streamlined glide in swimming with computational fluid dynamics methodology.

The importance of the flow effects around the swimmer has been introduced by Costa *et al*. (2015) wherein k–ε model of turbulence had been used to simulate fluid flow around the model and their results were validated with swimming pool experiments. Zhan (2015) in another research by using of 3D numerical simulation analysis evaluated passive drag near free surface by *RNG* k-ε turbulence model. His results have been conformed to mannequin towing experimental data.

The literature review shows that most numerical studies used k-ε model of turbulence for computational analysis even in hydrodynamic or aerodynamic problems, like the work of Wang *et al.* (2014) for computation of aerodynamic characteristic of three typical passenger vehicles in aerodynamic.

In this paper the swimmer motion has been modeled by *k-ε* model in order to drag forces calculation. The aim of this work is to specify how swimmer speed could be increased with auxiliary equipment without any risk according to CFD technique and by towing tank experimental outputs. Moreover the best minimum depth of swimmer motion and his power required has been determined.

2. MATHEMATICAL FORMULATION

Because of the turbulent nature of fluid around swimmer the most of the numerical methods are presented based on Reynolds-averaged Navier-stokes equations. In these equations the water-air interface are captured with the volume of fluid (*VOF*) method. The parameters in the presence of turbulence are included of mean and fluctuating components for each instantaneous variable. The time-averaging forms of the equations are as follow, (Wilcox 1994):

Continuity equation:

$$\frac{\partial}{\partial x_i}(\overline{U_\iota}) = 0 \tag{1}$$

Momentum equation:

$$\frac{\partial}{\partial x_j}\left(\rho\overline{U_\iota U_J}\right) = -\frac{\partial \bar{P}}{\partial x_i} + \frac{\partial}{\partial x_j}\left[\mu\left(\frac{\partial \overline{U_\iota}}{\partial x_j} + \frac{\partial \overline{U_J}}{\partial x_i}\right) - \rho\overline{u_\iota u_J}\right] \tag{2}$$

Where according to basic definition:

$$U_i(t) = U_i = \overline{U_\iota} + u_i \tag{3}$$

The value of each instantaneous component is sum of the mean or time average and fluctuating component at the same direction, i.e. velocity in Eq. (3). The last term of Eq. (2) is Reynolds stress tensor that is one of the unknowns that should be modeled for solving equations. According to Boussinesq approximation a suitable model might be in the following form:

$$-\rho\overline{u_\iota u_j} = \mu_t\left(\frac{\partial \overline{U_\iota}}{\partial x_j} + \frac{\partial \overline{U_j}}{\partial x_\iota}\right) - \frac{2}{3}\delta_{ij}\rho k \tag{4}$$

In this equation the parameter k is turbulent kinetic energy per unit mass and δ_{ij} is *Kronecker delta*. The standard *k-ε* model which is widely applied in CFD has been used to solve the system of equations. Of course, for solving problem two additional transport equations are required:

$$\rho\overline{U_\iota}\frac{\partial k}{\partial x_i} = \frac{\partial}{\partial x_i}\left[\frac{\mu_t}{\sigma_k}\frac{\partial k}{\partial x_j}\right] + \mu_t\left(\frac{\partial \overline{U_\iota}}{\partial x_j} + \frac{\partial \overline{U}_j}{\partial x_i}\right)\frac{\partial U_i}{\partial x_j} - \rho\varepsilon \tag{5}$$

$$\rho\overline{U_\iota}\frac{\partial \varepsilon}{\partial x_i} = C_1\,\mu_t\frac{\varepsilon}{\kappa}\frac{\partial U_i}{\partial x_j}\left(\frac{\partial \overline{U_\iota}}{\partial x_j} + \frac{\partial \overline{U_J}}{\partial x_i}\right) - C_2\,\rho\frac{\varepsilon^2}{\kappa} + \frac{\partial}{\partial x_i}\left[\frac{\mu_t}{\sigma_\varepsilon}\frac{\partial \varepsilon}{\partial x_i}\right] \tag{6}$$

The closure coefficients of *k-ε* model are:

$$C_1 = 1.44, \quad C_2 = 1.92, \quad \sigma_\kappa = 1.0, \quad \sigma_\varepsilon = 1.3$$

Where the turbulent viscosity μ_t is: $\mu_t = \rho C_\mu \kappa^2/\varepsilon$ and $C_\mu = 0.09$ (which is another coefficient of *k-ε* model).The parameter C_μ is viscosity modification factor in low Reynolds number near wall which will be given more accuracy in solution. All above coefficients are obtained by experiments in other widespread researches. After obtaining the forces that will be exerted on swimmer, i.e. drag force, the power required is calculated for overcome to it as follow:

$$P_r = D_t \,.\, U \tag{7}$$

In above equation D_t and U are total drag and free stream or in fact swimmer velocity. Generally, anybody could not be able to produce that power for speed more than 4.2 m/s stand alone and if anyone has been wanted to reach more speed then he should be used auxiliary equipment like *diver propulsion vehicle* (*DPV*). The swimmer should be resisted against this high hydrodynamic force value in high speed motion. Naturally the position of his head and legs is very important and in simulation they should be modeled accurately. On the other hand, if it was assumed that electrical power is going to be used for propelling him other parameters enter the problem, like propulsion efficiency (that is composed of propeller and motor efficiency) and weight geometry of such system. Thus the installed power P_i is defined for this condition as Eq. (8):

$$P_i = \frac{P_r}{\eta_p} \qquad (\eta_p = \text{propulsion efficiency}) \tag{8}$$

The hydrodynamic forces in underwater motion highly have been related to moving body shape and geometry. For example, there are strong separation at all sharp corners of rectangular cylinder that it will be caused very high drag force. While by rounding these sharp edges the drag will be reduced by about 45 percent though drag coefficient is still high. Nevertheless, the important part of the cylinder is the half rear end or cylinder trailing edge region which by streamlining this part to a quoin shape the pressure drag will be reduced 85 percent more than before for the given thickness. Therefore the aft body shape is very important to reduce drag force and for high-performance swimmer propulsion vehicles and other moving bodies the fore and aft shape of swimmer should be optimized for obtaining high speed underwater motion.

As mentioned above, the relative contribution of drag depends upon the body's shape and configuration. Generally the importance of body streamlining is needed to reduce drag at low speed (U≤3 m/s) to prevent swimmer overstress. But due to hydrodynamic pressure in high speed motion (U≥3 m/s) the swimmer's legs move to a fluid dictated position that coming from the nature of flow field and the body will be shaped automatically. Thus for reducing the power of swimmer in high speed motion the special helmet should be designed for him to take care of injury risk.

The depth motion of swimming is another important parameter that its' effects has been illustrated by

Vennell *et al.* (2006). They showed that the wave drag component will be increased about 2.4 times of total drag when the swimmer will come to near water surface. So the wave drag component would be expected to constitute a large proportion of their total drag in surface movement. In fact whatever he will be gone to deeper the effect of wave drag will be decreased and disappeared gradually and less power is needed to movement. Many researchers have been attempted to demonstrate exact value of wave drag experimentally and numerically too. For example, Vorontsov and Rumyantsev (2000) suggested that about 5% of wave drag in 2 m/s lesser than actual value. Toussaint *et al.* (1988) used a special measuring system (*MAD*) to estimate wave drag and they have been showed the greater contribution of wave drag, about 21% in 1.9 m/s. Wilson and Thorp (2003) have been used the power law fitting method to estimate about 10% to 20% of wave drag contribution relative to active drag in 1.0 m/s and between 35% to 45% in 2.0 m/s. One of the best results have been attained by Lyttle *et al.* (1998) as they presented the experiment results of 40 swimmers in different speeds from 1.6 to 3.1 m/s and different depths between zero to 0.6 m. They were understood that the drag force will be decreased about 20% in deep water in 2.2 m/s.

Therefore, if a swimmer wants to reach high speed motion without any wave drag in surface then he must go to deeper depth at least about 3 times of his equivalent diameter that will be computed from swimmer's frontal area (A_f) as:

$$A_f = \frac{\pi \cdot d_e^2}{4} \Rightarrow d_e = \sqrt{\frac{4\,A_f}{\pi}} \quad (9)$$

(d_e = Swimmer equivalent diameter)

$$h_s \geq 3d_e \ (h_s = \text{swimming depth}) \quad (10)$$

Experimental investigation of fluid dynamics around the swimmer in towing tank experiment is very difficult method because there is transient deformation of the swimmer body due to unsteady nature of the flow. So, the computational fluid dynamics modeling of swimmer may be one of the best ways to providing a tool for prediction of the flow field and for evaluating hydrodynamic characteristics. This allows to improving flow visualization and understanding of the swimmer behavior during the motion and observing high pressure regions around him precisely.

In this paper, the CFD method with k-ε turbulence model has been applied to demonstrate the flow field and for obtaining the drag force of swimmers. The realistic swimmers geometries have been modeled for simulation and the numerical calculation has been done for different speeds and depths. The experimental tests are performed by five different swimmers and one mannequin.

2.1. Data Reduction

The Reynolds and Froude numbers are the two primary non-dimensional parameters of concern regarding of flows under consideration. The first number must be taken into consideration when there are not any surface waves and as mentioned in Eq. (10) the swimmer is far enough from the free surface. Reynolds number is defined as:

$$R_e = \rho U L / \mu = U L / \upsilon \quad (L = \text{Swimmer length}) \quad (11)$$

Where in Eq. (11) the parameters U and υ are swimmer speed and flow kinematic viscosity. Generally, when the Reynolds number is higher than a critical value (for example 1.0e+6 for underwater tests) the flow is fully turbulent and the drag coefficient is constant thereafter. Similarly, when considering bodies with large scale flow separations the drag coefficient is reasonably independent of Reynolds number once a critical value is exceeded. In the case of complex shape such as a swimmer where many external protuberances are observed, there is less chance of this overall independence. As the swimmer might be exposed to a range of flow speeds it should be required to check the range of Reynolds Numbers to obtaining more complete prospect of the loads that the swimmer will be encountered in actual motion. The Reynolds numbers in our experimental tests are between 1.74e6 to 14.51e6 according to different swimmers size, which is more than critical value. The second number (Froude) is defined as:

$$F_r = \frac{U}{\sqrt{g.L}} \quad (U \text{ is swimmer speed}) \quad (12)$$

When the swimmer affects the free surface (like ships), this number will be become very important and there will be observed one or two critical values in humps drag. The characteristic length (L) can generally be selected conveniently; however the length that should be considered in this case is *the length of the swimmer when his hands are open and are in direction of his body*.

3. CONDITIONS AND FACILITIES OF TOWING TANK LAB

Diving test conditions might be varied considerably depending on water density whereas the temperatures fluctuated from around 4°C to 30°C. Consequently, the fluid properties also will be varied considerably. Thus for the purposes of assimilating to international tests it is clearly convenient to adopt some reference conditions in accordance with *ITTC 2006 Recommended Procedures and Guidelines*. These rules are based on fresh water in 20.9°C with a density value of 1024.364 kg/m^3. The kinematic viscosity υ in this temperature is 9.822e-7 m^2/s. In experimental tests the towing speed of swimmer should be varied considerably for obtaining favorable results. In this test the swimmer should be fixed in his position and applied identical conditions for each swimmer in towing tank test.

The swimmer's speed is about 3.8 m/s in commercial and sport situations which has been registered this condition by other researchers in experiments whereas the speed twice before has been considered here. However, because of lab limitation the speed not exceeded more than 7.8 m/s.

The experiments have been conducted in the pool with 140 m length, 3.5 m depth and 7 m width and

the towing force has been generated by using a 45 kilowatt electrical motor with inverter controller. In each case the temperature and density of water have been measured. The lab instruments supported the swimmer safely and by an industrial high speed computer the test data like drag force, acceleration and speed have been recorded. One underwater and two overwater cameras have been used for capturing the situations of the swimmers during each experiment.

The dimensions of towing tank are large enough to avoid flow blockage effects. Namely, the tank cross section compared to swimmer cross section is large enough whereas it has been satisfied the *ITTC 2002 rules*. The swimmers frontal areas are approximately between 0.0872 to 0.11 m^2 and the pool cross sectional area is 22.5 m^2, so the blockage ratio is suitable for experimental tests.

3.1. Experimental Procedures

The swimmers have been towed by a handle bar mounting under water which it is attached to the bottom of moving carriage with a load cell. As the carriage accelerates, drag measurements will be recorded across the whole speed range of interest and the speed has been registered from an encoder wheel that is attached to the carriage. All data were acquired by using a PC based *National Instrument* data acquisition system that has been sampled at 100Hz rate. The output data have been averaged in order to eliminating the effects of any unsteadiness and unfavorable noise and the averaged values have been stored for further analysis and comparison with numerical outputs.

The test is started whenever the swimmer holds his breath and the measuring are started now. The test and measuring was continued until he released the towing handle. The swimmer safety could be attained with this voluntary decision. As shown in (Fig. 1) the image of whole swimmer body has been captured with a water proof camera during the tests.

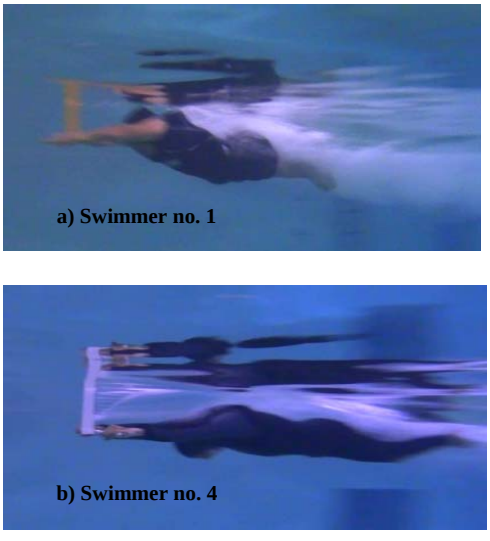

Fig. 1. Swimmers configuration in towing tests, a) Swimmer speed 7.6 m/s – b) Swimmer speed 4 m/s.

The tests will be done with the same conditions with a mannequin again, (Fig. 2). The only deviation is the mounting attachment configuration.

Fig. 2. Mannequin deep water test in towing tank lab, speed 7.6 m/s.

Whereas the swimmer is supported by a handle bar in the test its' effect should be established and the data would be corrected according to superposition method to determine the swimmer drag alone. The handle bar should be tested individually without swimmer in order to obtain its' interference effect. Using this method, the contribution of the handle bar to the total drag could be determined. This method of correction allows to determining direct contribution of the support and the interference effect of the support to the swimmer. The support is made of thin section bar with rounded leading edge and trailing edge to minimize the handle bar undesirable effects. Although the pylon is capable of providing trim, heave and drag force, though in this case the study is limited to drag force measuring.

4. NUMERICAL METHOD

The numerical simulations were carried out by the ANSYS Fluent commercial CFD code. This code is based on the Patankar (1980) finite volume method to solve the system of equations governing the fluid flow around the model.

4.1. Swimmer Geometry and Modeling

The surface model of each swimmer was generated by 3D image processing with moving possibility of each part with digital mock up. Then the surfaces were assembled with many joints. The angle of each element has been easily changed to setting an accurately equal angle with the actual model. This configuration is shown in (Fig. 3) for swimmer no. 4 typically. Half of the model was considered in symmetric coordinate to provide a model of numerical analysis with less calculating time.

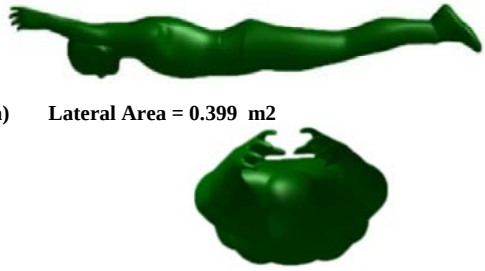

a) Lateral Area = 0.399 m2

b) Frontal Area = 0.11 m2

Fig. 3. Software model for numerical analysis of swimmer no.4 typically.

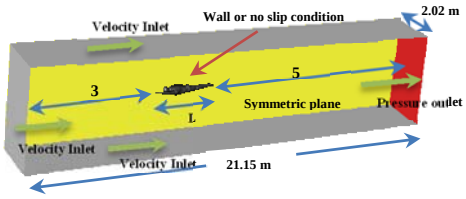

Fig. 4. Calculating domain and boundary conditions (swimmer no.4).

4.2. Calculating Domain and Grid Generation

The size of the solution domain was chosen with respect to another experience in cylinder simulation and test for selecting its' suitable size. This size is about 9 times the model length with open arms (3 times upstream and 5 times downstream) and the width is 9 times of his shoulder width (4 times each side). This domain with its boundary condition has been shown in (Fig. 4). The grid has been generated with quadratic structured type over the whole domain but for more accuracy the grid has been so fined adjacent to the model body with pyramidal un-structured type, (Fig. 5). The aspect ratio of cells in overall domain is less than 5 near body and less than 20 far from it.

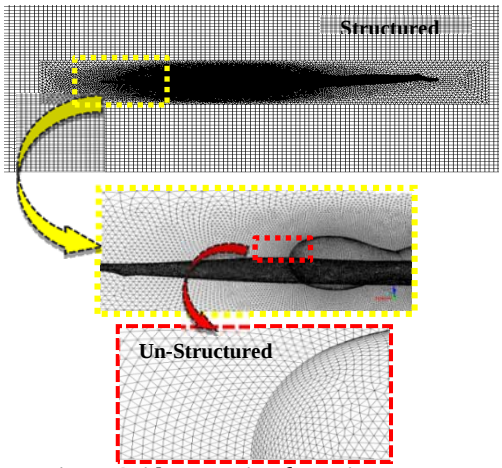

Fig. 5. Grid generation for swimmer no.4.

4.3. Grid Study

Although by three methods of turbulence (*k-ε* and *k-ω* and *Reynolds-Stress*) the results of grid study would be obtained for a typical swimmer but for brevity and because of no major differences that take place between them the output results of *k-ε* model are presented hereafter. The grid study was done with 1.4e6, 3.03e6, 4.5e6 and 6.1e6 cells and the results compared in Table 1.

This table shows that to obtaining accurate output by saving computational time the grid 4.5e6 cells with respect to 6.1e6 cells had no significant difference, so this grid is selected. The convergence criterion of solution quantities (continuity- X velocity- Y velocity- Z velocity- turbulent kinetic energy k – dissipation rate ε – volume of fluid vf) are chosen as equal to 1e-5.

Table 1 Grid sensitivity study

U=10 m/s h_s=0.35m	Comparison of Drag force respect to solution time			
Number of Grid	1.4e6	3.03e6	4.5e6	6.1e6
Drag Force (N)	2354.18	2161.84	2036.67	2035.04
Percent of Difference	8.17%		5.79%	0.08%
Solution time	18 Hour	1.5 day	3 Day	4.5 day
Convergence Criterion : 1e-5				

5. RESULTS AND DISCUSSION

The first parameter that needs to be checked is Y^+ which must be less than 100 for *k-ε* method (Fig. 6). The law of the wall that has been known as Y^+ is a dimensionless distance from the wall surface and it should be appropriated value to get the acceptable solution.

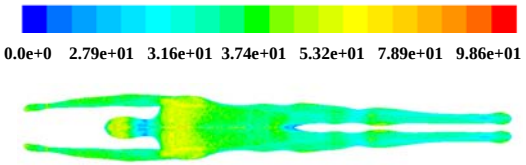

Fig. 6. The swimmer body contours of Y^+.

The contour of static pressure on symmetry plane and on swimmer body at the velocity of 7.6 m/s and depth of 0.1 m is indicated in (Fig. 7). There are many low pressure regions around the swimmer body like head and shoulder that is due to accelerating of flow in this region. The swimmer's eyes and ears should be resisted against this high or even low fluid pressure. It has been tried to keep the time of test as short as possible in real test until the swimmer has not been needed any special swimmer suit. Moreover, the high pressure region takes place ahead of stream, which makes a stagnation point zone and each swimmer should be protected of his neck against this high pressure value.

The deformation of wave at various depths has been shown in (Fig. 8). In that figure the distance between hollow and bump is about 0.361 m for moving depth of 0.35 m, and 0.479 m for moving depth of 0.22 m and 0.716 m for moving depth of 0.10 m, which means that whenever the depths are decreased the wave height will be increased and vice versa. The wave is approximately disappeared for more depth over 0.6 m. The additional pictures of experiment for the hump wave formation have been presented in (Fig. 9).

In Table 2 the size and body specifications of all swimmers with their maximum total drag has been

adduced. The variation between total drag values arises from many parameters such as frontal area, swimmer head and legs and body position. The data from this table enables us to select the best swimmer between them according to swimming style and his ability for continuing high speed test.

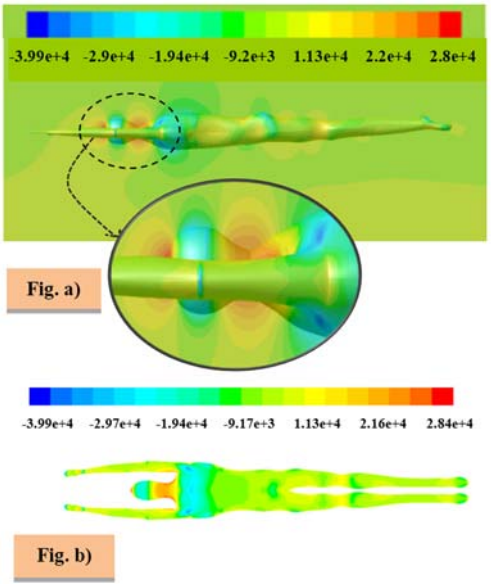

Fig. 7. The contour of static pressure in 0.1 m depth and 7.6 m/s speed; a) in symmetric plane, b) on body.

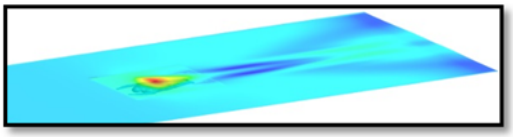

Fig. 8. The wave formation in z-coordinate, U= 7.6 m/s, h_s= 0.1m, Wave Height= 0.716 m.

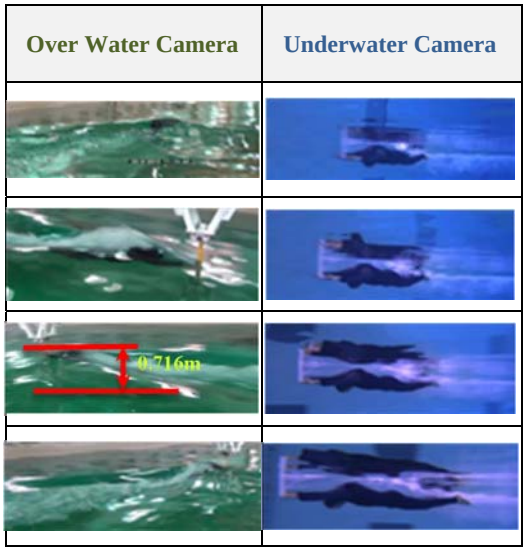

Fig. 9. The hump wave formation in free surface top of swimmer body.

On the other hand the numerical simulation showed the similar trend to actual test without any additional torsion around the swimmer body as is (Fig. 10).

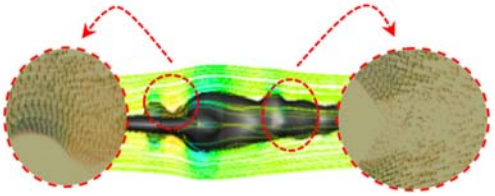

Fig. 10. Path line around swimmer no. 4, head region and tail region vector line.

In (Fig. 10), vector line of head region and tail region of the swimmer's body has been presented. The single circulation zone is observed behind the body just between the legs of swimmer in a small region that causes further drag, to reduce it the swimmer must attach his legs to each other. As predicted the drag–velocity curve at depth of 0.35 m shows the drag increase with the velocity, (Fig. 11), and in fact, the outputs smooth reasonably.

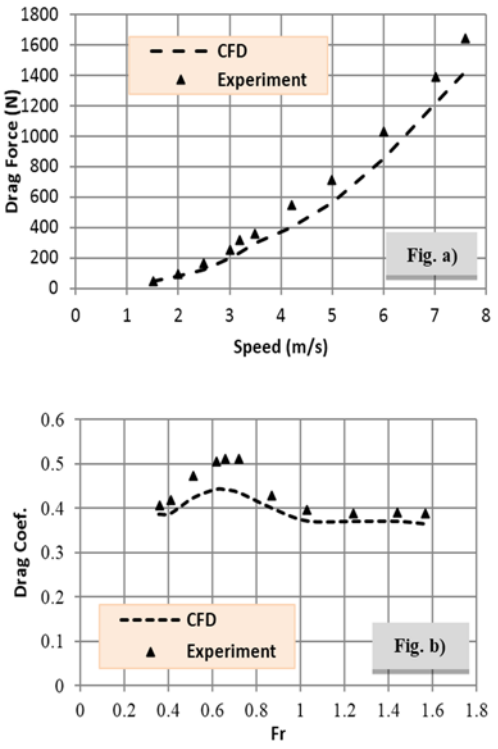

Fig. 11. Swimmer no.4 in 0.35 m depth a) Drag force vs. velocity b) Drag coefficient vs. Froude no.

In this figure a typical hump occurred in speed between 2.5 and 4 m/s that was induced us to take more data (both test and computation) in this interval. The moving of the free surface wave concomitant by the swimmer with the same speed is physical justification of this behavior. It means that an increasing of total drag has been occurred and more power will be needed to dominate this resistive force. When the swimmer's speed is going to be increased his body more adapted and will be formed to flow field and encounter to lesser wave which will be caused to reduce total drag thereafter. Besides, if the swimmer goes to more depth the wave will be

Table 2 Swimmer's characteristics and their total drag in velocity of 7.6 m/s

Swim. / Spec.	1	Mannequin	2	3	4	5
	Depth = 0.90 m		Depth = 0.35 m			
Height (cm)	182	180	176	190	183	171
Head circum. (cm)	57	57	53	60	57	55
Waistline (cm)	96	96	93	94	88	86
Arm length (cm)	80	-	80	90	83	80
Shoulder width (cm)	50	50	46	52	48	45
Frontal area (m^2)	0.11	0.11	0.101	0.115	0.11	0.077
Weight (kg)	87.8	87	77.5	97.7	83.4	74
Max Drag (N)	1951.8	1898.8	1298.8	1341.8	1155.4	1281.4

slowly disappeared. Also, tests in low depths with low velocity indicate oscillation in output results and more interaction with the surface water and swimmer take place, whereas in high depths this interaction is weak. The same trend is observed for other depths, for example, in (Fig. 12) for depth of 0.9m. In this figure the numerical computation has accurately accordance to test results. The free surface in this depth is not affected by swimmer motion and any wave drag has not been occurred. For this reason the swimmer motion near surface has more drag relative to motion in deep water. These results are indicated in (Figs. 11 and 12).

The same event has been occurred to swimmer no. 4 when he approached the surface and the wave drag had increased the total drag about 83% in speed 3.2 m/s, (Fig. 13). The operation recognition of this important event in water movement is very important and should be reduced its undesirable effect in high speed motion. It could be happened by increasing depth motion, moving head just between his hands and reducing head angle and straightening his waistline.

The drag–velocity curves exhibit a smooth second order behavior that approaches to maximum 1176.57N in 7.6 m/s in 0.35m depth. In this speed the power required to overcome to swimmer resistive force is about 9.8Kw according to Eq. (7) and in speed 10 m/s this power is predicted to be about 22.7Kw. If he goes to 0.9m depth the drag force is equal to 1687.5N in 10m/s that will comprise more 21% decrease in drag force. If the swimmer wants to reach this speed he must be produced high power which it is impossible by him alone and if he wants to reach this speed he should be used an external swimmer propulsion vehicle. Though the use of propulsion equipment has been created more problems to him, like its weight, volume, its excess drag and etc. that should be solved each one. If an electrical propulsion system is going to be used with propulsion efficiency of 75% (for propeller and electrical motor) the power capacity that should be installed is equal to 30.2Kw. Really this is constituted of huge equipment for a person to carry and use it. It is very important to reach this performance under water and obtain a new recording speed which is the future aim of author research.

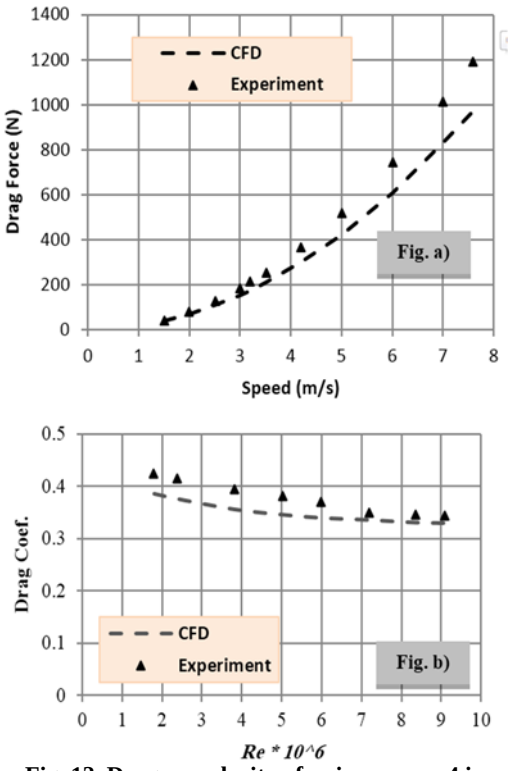

Fig. 12. Drag vs. velocity of swimmer no. 4 in 0.9m depth, a) Drag force vs. velocity, b) Drag coefficient vs. Reynolds number.

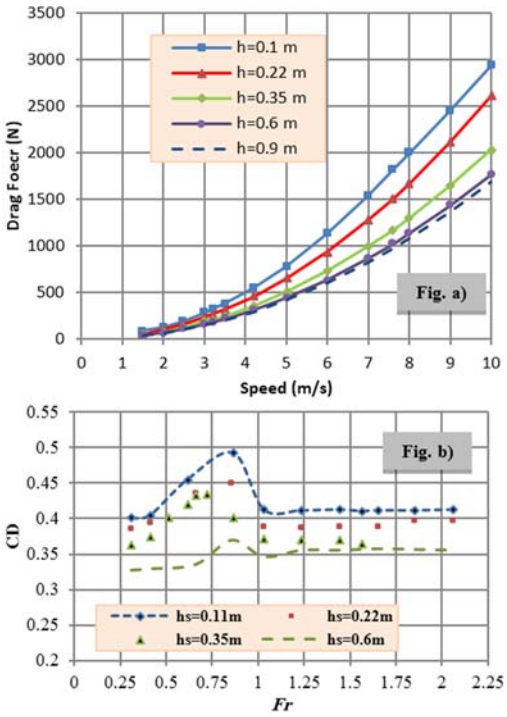

Fig. 13. a) The drag vs. velocity, b) Drag coefficient vs. Froude number for swimmer no. 4 in various depths from CFD.

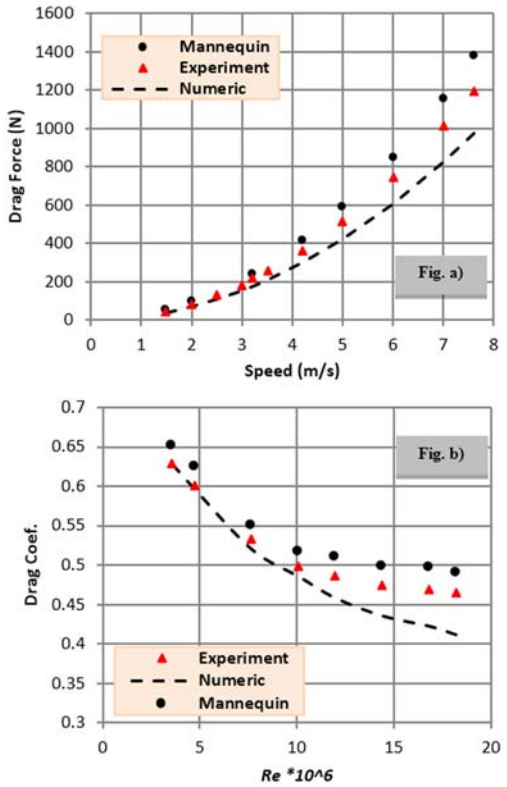

Fig. 14. Numerical and experimental results of swimmer no. 1 and mannequin, a) Drag force vs. velocity, b) Drag coefficient vs. Froude no.

The comparison of swimmer 1 and the mannequin has been shown in (Fig. 14). The curves are approached to each other in low speed tests while with increasing speed the deviation of outputs have been increased. The deformation on swimmer shoulder against fixed size of mannequin shoulder in high speed motion and different pylon attachment position is justification of these deviations. This deviation is shown better in dimensionless curve of (Fig. 14 b).

6. CONCLUSION

The aim of this paper was to simulate swimmer motion in high speed based on reliable method. The numerical output results have been validated by towing tank experiment. In the past the same work has been done for lesser swimmer speed up to 3.8 m/s by researchers while in this research the speed of swimmer has been increased at least twice (7.6 m/s) both in simulation and in real test especially. Moreover the ability of swimmer is being predicted for designing a high speed swimmer propulsion vehicle. For this investigation the computational fluid dynamic based on k-ε method of turbulence has been used to compute drag force and the power required in succedent. The validity has been investigated by using experiments and the effects of speed and depth variation are considered, too.

Though the three models of turbulence were applied for computation, for compendium only the result of k-ε method has been reported. The measurements showed that total drag has been increased rapidly by increasing speed. The experimental drag force results showed the same trend with numerical simulation and only a slight deviation may be seen in high speed when the swimmer body has been deformed transiently during the test. In fact by this deformation the real frontal area of the swimmer has been reduced and it has been caused to reduce total drag. The experiments on 5 swimmers and one mannequin have been given suitable statistic set to evaluate more accurate prediction about hydrodynamic drag coefficient in different speeds and depths. Furthermore the reliability of the CFD output results has been shown in this paper. The designing of auxiliary power equipment for increasing swimmer/diver speed is being continued based on these outputs.

The magnitudes of drag forces showed that total drag at the surface is higher than the drag when swimmer fully immersed. This additional drag is due to the energy required to form waves that are generated in free surface. On the other hand, in high speed motion because of the normal force acting on swimmer body, this will be better body reconfigured to flow stream lines and induce relatively lower drag force in real experimental test. Actually, this event (deformation of the body during the test) was not simulated. However, the result showed 137% increase in total drag that has been take place when the swimmer comes near the surface.

Of course, the swimmer required net power is about 22.3 Kw (with considering system efficiencies this power is about 32kw) in speed of 7.6m/s that no one can be produced it alone and complementary accessories should be used. Nevertheless, the swimmer physical ability should be equaled to hydrodynamic drag to keep

him in high speed motion and in long time. Furthermore, to reach the highest speed it is better for him to swim at least 0.9 m depth that has minimum drag. It seems that the swimmer withstands to related drag up to 8 m/s but if he will be want to reach 10 m/s, a special swimsuit with head protection is necessary.

In summary in order to increasing swimmer speed, the minimum drag force in suitable depth has been attained for some swimmers in numerical simulation and they have been validated by experimental method. Actually with this study the computational ability of estimating forces on swimmer has been established in high speed motion. Moreover the total power related to each speed has been evaluated for each swimmer. According to this parameter the battery capacity and overall dimension of swimmer thruster unit will be obtained for future research.

This research will be continued in order to designing the equipment or accessories of the swimmer to be enabled him to reach the speed of 10 m/s.

REFERENCES

Bixler, B. S. and M. Schloder (1996). Computational Fluid Dynamics: An analytical tool for the 21st century swimming scientist. *Journal of Swimming Research* 4-22.

Bixler, B. S. and S. Riewald (2002). Analysis of Swimmer's Hand and Arm in Steady Flow Conditions Using Computational Fluid Dynamics. *Journal of Biomechanics* 35, 713–717.

Cohen, R. C. Z (2009). Simulation of Human Swimming Using Smoothed Particle Hydrodynamics. In *proceeding of Seventh International Conference on CFD*, CSIRO, Melbourne, Australia.

Costa, L. (2015). Computational fluid dynamics vs. inverse dynamics methods to determine passive drag in two breaststroke glide positions. *Journal of Biomechanics* 48(10), 2221-2226.

Gardano, P. and P. Dabnichki (2006). On Hydrodynamics of drag and lift of the human arm. *Journal of Biomechanics* 39, 2767–2773.

ITTC (2002). *Recommended Procedures and Guidelines*. Testing and Extrapolation Methods for Resistance Test, 7.5-02-02-01 and Blockage Corrections, 3.6.3 page 8.

ITTC (2006). *Recommended Procedures and Guidelines* Edited by 22nd *ITTC QS Group* for Testing and Extrapolation Methods, 7.5-02-01-03 and General Density and Viscosity of Water, Values of Mass Density for Salt Water, page 4 table 2.

Lyttle, A. D. (1998). The Effect of depth and velocity on drag during the streamlined glide. *Journal of Swimming Research* 13, 15–22.

Marinho, D. A. (2009). Hydrodynamic drag during gliding in swimming. *Journal of Applied Biomechanics* 25(3), 253-257.

Marinho, D. A. (2011), Three-dimensional CFD analysis of the hand and forearm in swimming. *Journal of Applied Biomechanics* 27, 74-80.

Patankar, S. V. (1980). In: *Numerical heat transfer and fluid flow*. Hemisphere, New York.

Popa, C. V. (2011). Analysis of wall shear stress around a competitive swimmer using 3D Navier–Stokes equations in CFD. *Acta of Bioengineering and Biomechanics* 13(1), 3-11.

Ramos, R. (2012). The effect of body positions on drag during the streamlined glide: A Three-dimensional CFD analysis. In *Proceeding of 18th Congress of the European Society of Biomechanics, Journal of Biomechanics*.

Rouboa, A. (2006). The effect of swimmer's hand/forearm acceleration on propulsive forces generation using computational fluid dynamics. *Journal of Biomechanics* 39, 1239–1248.

Sato, Y. T. Hino (2003). Estimation of thrust of swimmer's hand using CFD. In *Proceedings of the Second International Symposium on Aqua Bio-Mechanisms*, Honolulu, Hawaii, USA 71–75.

Toussaint, H. M. (1988). Propelling efficiency of front crawl swimming. *Journal of Applied Physiology* 65, 2506–2512.

Vennell, R., D. Pease and B. Wilson (2006). Wave drag on human swimmers. *Journal of Biomechanics* 39(4), 664-671.

Vorontsov, A. R. and V. A. Rumyantsev (2000). Resistive forces in swimming. In *Biomechanics in Sports*: *Performance Enhancement and Injury Prevention.* Vol. IX Encyclopedia of Sports Medicine, Blackwell, IOC Medical Commission.

Wang, Y., Y. Xin, Z. Gu, S. Wang, Y. Deng and X. Yang (2014). Numerical and experimental investigations on the aerodynamic characteristic of three typical passenger Vehicles. *Journal of Applied Fluid Mechanics* 7(4), 659-671.

Webb, A. (2011). Prediction of passive and active drag in swimming. In *Proceeding of 5th Asia-Pacific Congress on Sports Technology (APCST)*. Elsevier science direct.

Wilcox, D. C. (1994). *Turbulence Modeling for CFD.*

Wilson, B. D. and R. Thorp (2003). Active drag in swimming. In: J. C. Chatard and Puget, J. M. (Eds.), *Proceedings of the IX World Symposium. Biomechanics and Medicine in Swimming*, St Etienne, 21–26.

Zaidi, H. (2010). Turbulence model choice for the calculation of drag forces when using the CFD method. *Journal of Biomechanics* 43(3), 405-411.

Zhan, J. M. (2015). 3D numerical simulation analysis of passive drag near free surface in swimming. *China Ocean Engineering* 29, 265-273.